Geophysical Research Letters

RESEARCH LETTER
10.1029/2018GL079686

Key Points:
- The trend of tropical cyclone migration over the western North Pacific reversed during the recent warming slowing-down period (after ~1999)
- It is the change of regional sea surface temperature that contributed greatly to the meridional migration trend of tropical cyclones
- The effect of regional sea surface temperature change came from its impact on storm potential intensity and large-scale circulation

Supporting Information:
- Supporting Information S1
- Data Set S1
- Data Set S2

Correspondence to:
T. Li,
timli@hawaii.edu

Citation:
Sun, Y., Li, T., Zhong, Z., Yi, L., Chen, X., Ha, Y., et al. (2018). A recent reversal in the poleward shift of western North Pacific tropical cyclones. *Geophysical Research Letters*, *45*, 9944–9952. https://doi.org/10.1029/2018GL079686

Received 19 JUL 2018
Accepted 30 AUG 2018
Accepted article online 4 SEP 2018
Published online 19 SEP 2018

A Recent Reversal in the Poleward Shift of Western North Pacific Tropical Cyclones

Y. Sun[1,2], T. Li[1,3], Z. Zhong[2,4], L. Yi[5], X. Chen[2], Y. Ha[2], J. Zhu[1], Y. Shen[2], Z. Xu[1], and Y. Hu[2]

[1]Key Laboratory of Meteorological Disaster, Ministry of Education/Joint International Research Laboratory of Climate and Environmental Change/Collaborative Innovation Center on Forecast and Evaluation of Meteorological Disasters, Nanjing University of Information Science and Technology, Nanjing, China, [2]College of Meteorology and Oceanography, National University of Defense Technology, Nanjing, China, [3]IPRC and Department of Atmospheric Sciences, University of Hawai'i at Mānoa, Honolulu, HI, USA, [4]Jiangsu Collaborative Innovation Center for Climate Change, School of Atmospheric Sciences, Nanjing University, Nanjing, China, [5]Chinese Academy of Meteorological Sciences/Chinese Meteorological Society, Beijing, China

Abstract Recent studies have revealed a global, poleward migration trend of tropical cyclones (TCs) in terms of annual-averaged latitude of lifetime maximum intensity under the global warming. The TCs in the western North Pacific (WNP) make the largest contribution to this trend. One existing hypothesis is that there is a linkage between poleward migration of TCs and anthropogenic forcing. Here we introduce a new measurement, the lifetime-averaged latitude weighted by TC destructive potential, to detect the meridional migration of the WNP TCs, which is more reliable and meaningful as it considers not only past data uncertainty but also public concerns. Our results show that the trend of WNP TC migration reversed during the recent warming slowing-down period (after ~1999). Different from the existing hypothesis, it is the change of regional pattern of sea surface temperature that contributes greatly to the meridional migration of WNP TCs.

Plain Language Summary Tropical cyclones (TCs) account for the majority of natural catastrophic losses in the developed world and are the second leading cause (next to floods) of death and injury among natural disasters affecting developing countries. The challenges for climate detection and attribution research with regard to TCs are to determine whether an observed change in TC activity exceeds the natural variability and to attribute significant changes to anthropogenic forcing (e.g., greenhouse gases or aerosols). Recent studies have indicated that the TCs over the western North Pacific (WNP) systematically migrated poleward, which is plausibly linked to the expansion of the tropics associated with anthropogenic forcing. However, utilizing our new measurement, we find that the poleward migration of WNP TCs reversed direction during the recent warming slowing-down period (after ~1999). We thus propose a new mechanism associated with the regional pattern of sea surface temperature change, which is characterized by a relatively warm or cold sea surface temperature pool in the region (20–40°N, 140–160°E). Compared with the previous theory based on anthropogenic forcing and well-known dominant modes of variability, the new mechanism provides a more convincing explanation for the migration of WNP TCs since 1980, especially for the recent warming slowing-down period.

1. Introduction

Against the background of climate change and considering the catastrophes and economic damages caused by tropical cyclones (TCs), it is of societal importance and great scientific interest to understand whether and how global warming may have already affected TC activities over the oceans (Lee et al., 2012). However, relatively little is known about the impact of global warming on TC tracks (Wang et al., 2011), despite many progresses assessing the possible changes in TC intensity and its potential destructiveness (Knutson et al., 2010).

During the past decades, the average location where TCs reached their lifetime maximum intensity (LMI) systematically shifted poleward in the Northern and Southern Hemispheres by 53 and 62 km/decade, respectively (Kossin et al., 2014). As the most active basin of TC frequency, the TCs in the western North Pacific (WNP) made the largest contribution to the poleward migration trend in the Northern Hemisphere (Kossin et al., 2016, 2014). Results of several model projections suggested that the poleward shift of the

TCs in the WNP would continue over the 21st century (Kim et al., 2011; Kossin et al., 2016, 2014; Murakami et al., 2012; Wang et al., 2011; Wu & Wang, 2004; Ying et al., 2012; Yokoi & Takayabu, 2009), which would potentially have profound impacts on people's lives and properties. Increasing mortality risks and hazard exposures from TCs (Peduzzi et al., 2012) may be compounded in coastal cities outside the tropics, while they may possibly be offset at lower latitudes (Cardona et al., 2012; Kossin et al., 2016).

Due to the large natural variability in TC activity over the WNP (Chan & Shi, 1996; Liu & Chan, 2008) and the difficulty of quantifying the contribution to TC track changes by natural variability with relatively short observation records (Kossin et al., 2014), it remains unclear whether the observed TC track changes are linked to global warming (Knutson et al., 2010; Lee et al., 2012; Wang et al., 2011), let alone the impact of the recent warming hiatus (Fyfe et al., 2013; Kosaka & Xie, 2013; Li et al., 2015; Meehl et al., 2014; Trenberth & Fasullo, 2014) on the TC tracks over the WNP. The prevailing poleward shift of TCs is generally attributed to the expansion of the tropics associated with global warming (Kossin et al., 2016, 2014; Murakami et al., 2012; Wu et al., 2014), but the mechanisms are not yet agreed on.

Here we focus on the period of 1980–2016, which contains both a rapid warming (RW) period (1980–1999) and a warming slowing-down (WS) period (1999–2016). Note that the recent WS period includes not only the warming hiatus period (1999–2013) (Fyfe et al., 2013; Kosaka & Xie, 2013; Li et al., 2015; Meehl et al., 2014; Trenberth & Fasullo, 2014) but also the years of 2014–2016 as the global temperatures in 2014–2016 were warmer than normal especially in 2015 and 2016, according to the Global Land-Ocean Temperature Index (available at https://www.esrl.noaa.gov/psd/gcos_wgsp/Timeseries/GLBTSSST/). During this period (1980–2016), the best track data are considered most complete and at their highest quality in terms of both storm location and storm intensity thanks to geostationary satellites (Dee et al., 2011; Kalnay et al., 1996; Knapp & Kruk, 2010; Kossin et al., 2014). We expand on previous studies (Kossin et al., 2016, 2014) by analyzing observations of the TC best track data and sea surface temperature (SST) data and focus on the difference in large-scale steering flows of TCs and thus TC migrations over the WNP between RW and WS periods.

2. Materials and Methods

The best track data include the International Best Track Archive for Climate Stewardship (IBTrACS) v03r10 (Knapp et al., 2010; available at http://www.ncdc.noaa.gov/ibtracs/). For the WNP TCs, there are four best-track data sets from four different agencies: the Joint Typhoon Warming Center, the Japan Meteorological Agency, the China Meteorological Administration, and the Hong Kong Observatory. The SST data are from the U.S. National Oceanic and Atmospheric Administration (NOAA) Extended Reconstruction of SST (Smith & Reynolds, 2003), which is a global gridded reconstructed data set based on historical, observed SST data using statistical methods.

The El Niño–Southern Oscillation (ENSO), Pacific Decadal Oscillation (PDO), Interdecadal Pacific Oscillation (IPO), and relative SST (defined in section 4) variability were removed from the annual-mean φ_{DP} time series by regressing individual φ_{DP} time series from each best track data set onto the indices of the Niño-3.4, PDO, tripole IPO (Henley et al., 2015), and relative SST, respectively, and analyzing the residuals ($\varepsilon_{Niño\text{-}3.4}/\varepsilon_{PDO}/\varepsilon_{IPO}/\varepsilon_{RSST}$). We also analyze residuals of the trivariate regression of φ_{DP} onto the Niño-3.4, PDO, and tripole IPO indices (i.e., ε_{N+P+I}) when the ENSO, PDO, and IPO variabilities were all removed from the φ_{DP} time series. For detailed regressing method, readers are referred to Kossin et al. (2014). Monthly indices of Niño-3.4, PDO, and tripole IPO are provided by the National Oceanic and Atmospheric Administration's Earth System Research Laboratory Physical Sciences Division (Mantua et al., 1997; Rayner et al., 2003; available at http://www.esrl.noaa.gov/psd/gcos_wgsp/Timeseries/). Here annual averages of the WNP-mean SST, ENSO (Niño-3.4), PDO, IPO (tripole IPO index), and relative SST indices are taken over June–October, which is regarded as the peak TC season (Yang et al., 2015).

3. Results

3.1. Trends of TC Migration Over the WNP During Different Warming Periods

The measurement of TC latitude at the time of LMI, φ_{LMI}, is comparatively robust to the heterogeneities introduced into the best track data by both temporal inconsistency in data quality and analysis as well as interagency procedural differences (Kossin et al., 2014). Thus, we first use φ_{LMI} to detect the meridional

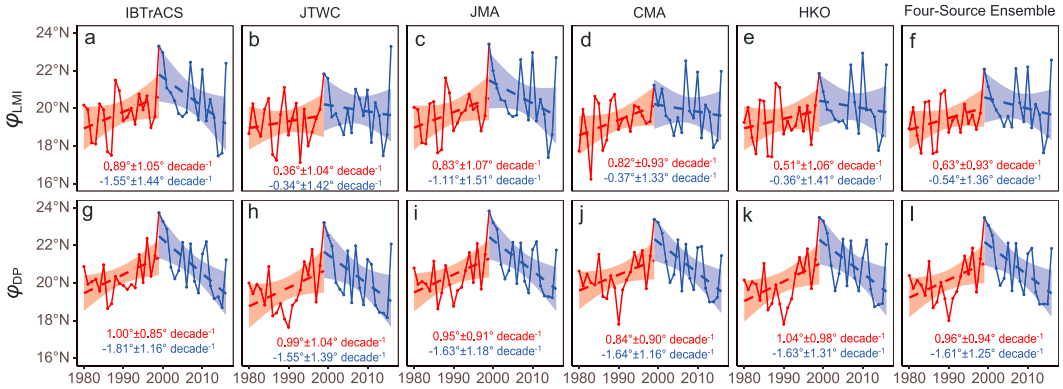

Figure 1. Meridional migrations of WNP TC during the RW (red color) and WS (blue color) periods. Time series of annual-mean latitude of LMI (φ_{LMI}; a–f) and latitude weighted by TC destructive potential (φ_{DP}; g–l) over the WNP calculated from various best track historical data. Linear trends (dashed lines) are shown with their 95% two-sided confidence intervals (shading), which are also quantitatively presented (annotated values). WNP = western North Pacific; TC = tropical cyclone; RW = rapid warming; WS = warming slowing-down; LMI = lifetime maximum intensity; IBtrACS = International Best Track Archive for Climate Stewardship; JTWC = Joint Typhoon Warning Center; JMA= Japan Meteorological Agency; CMA = China Meteorological Administration; HKO = Hong Kong Observatory.

migration trend of TCs over the WNP. Because of the short period after 1980, the estimated φ_{LMI} trend is highly sensitive to the sample size. Take the IBTrACS best track data, for example, when the focus period changes from 1980–2013 to 1980–2016, the trend first decreased from 1980–2012 to 1980–2015 due to the relatively low φ_{LMI} in 2014 and 2015 and then increased during 1980–2016 (Table S1 in the supporting information). This raises a question about the observed poleward shift of TCs over the WNP in the past decades.

As some portion of the φ_{LMI} trend is assumed to be linked to the expansion of the tropics caused by global warming (Allen et al., 2012; Kossin et al., 2014; Wu et al., 2014), the trend is projected to be different in the recent WS period. As expected, a significant, abrupt decadal change occurred in 1999 based on the IBTrACS data set, which is consistent with the beginning of the recent WS period as the abrupt decadal change of the averaged WNP SST in 1999 was significant at the 99% confidence level (Figure S1). Thus, we investigate different trends of TC migration in the RW and WS periods, respectively. Note that although the estimated overall trends of φ_{LMI} are basically consistent among different best track data sets, there are relatively large differences in φ_{LMI} among these best track data sets (Figures 1b–1f and S2). This implies that φ_{LMI} may not be as certain as expected, because the time when a TC reached its LMI is somewhat uncertain, especially for the TC with more than one intensification period.

We design a new measurement, the lifetime-averaged latitude weighted by TC destructive potential (φ_{DP}), to detect the meridional shift of TCs over the WNP. The new measurement considers not only uncertain factors but also public concerns (i.e., TC destructive potential). As the destructive potential can be estimated by integrating the cube of maximum wind speed over its lifetime (i.e., power dissipation index or PDI; Emanuel, 2005), φ_{DP} of a TC and annually averaged φ_{DP} ($\varphi_{DP\text{ - annual}}$) are given by the following:

$$\varphi_{DP} = \frac{\int_0^\tau \varphi \cdot V_{max}^3 dt}{\int_0^\tau V_{max}^3 dt} = \frac{\int_0^\tau \varphi \cdot V_{max}^3 dt}{PDI} \quad (1)$$

$$\varphi_{DP\text{-annual}} = \frac{\sum_1^N (\varphi_{DP} \cdot PDI)}{\sum_1^N PDI} = \frac{\sum_1^N \int_0^\tau \varphi \cdot V_{max}^3 dt}{\sum_1^N \int_0^\tau V_{max}^3 dt} \quad (2)$$

where τ is the lifetime of TC, V_{max} is the maximum surface wind speed, and φ is the latitude of TC center. Note that, to consider the contribution of weak TCs, the definition of PDI in this study is somewhat different from the PDI definition in Emanuel (2005), as ours considers all wind speeds while Emanuel's only considers the wind speed exceeding 17 m/s in the best track data set. φ_{DP} is a reliable measurement with little uncertainty for the following four reasons. First, similar to φ_{LMI}, φ_{DP} is also insensitive to the usual temporal heterogeneity of intensity estimate because it is determined by relative intensity during TC lifetime rather than by the

uncertain absolute value of TC intensity. Second, φ_{DP} considers the whole lifetime of TC rather than an instantaneous moment in φ_{LMI}, which is much uncertain in some TC cases (Figure S3). Third, φ_{DP} is not sensitive to the moments of cyclogenesis and cyclolysis, which are greatly different among various best track data sets (see Figure 3 in Kruk et al., 2010). As φ_{DP} is closely related to the TC destructive potential, which is estimated by the cube of maximum wind speed during the lifetime of TC, the periods (initial and final TC periods) when the TC is weak contribute little to φ_{DP} (Figure S4 and Tables S2 and S3). Fourth, the annual-averaged φ_{DP} is not sensitive to the estimate of weak TC number. Due to differences in criteria used to identify TCs, some weak TCs with little public concerns may be identified by some agencies but not by the other agencies. This inconsistency may contribute remarkably to the uncertainty of φ_{LMI} due to the importance of weak TCs to φ_{LMI} (Zhan & Wang, 2017) and only play a minor role in determining the annual-mean φ_{DP} that is largely determined by the strong TCs with large PDI according to equation (2) (Figure S5 and Table S4). In this study, φ_{DP} exhibits much less uncertainty than φ_{LMI}, as the difference in φ_{DP} trends among various best track data sets (0.08°/decade in RW period and 0.10°/decade in WS period) is much smaller than that in φ_{LMI} trends (0.23°/decade in RW period and 0.56°/decade in WS period) in terms of standard deviation (Figures 1g–1l), and the standard deviation of φ_{DP} among various best track data sets is significantly smaller than that of φ_{LMI} at the 95% confidence level (Figure S2). Therefore, compared with φ_{LMI}, φ_{DP} is insensitive to heterogeneities in the best track data sets and thus is a more reliable and reasonable measurement for investigating the meridional shift of TCs.

Over the whole study period (1980–2016), the estimated φ_{DP} trend, which is not sensitive to the changes in number and latitude of weak TCs as mentioned above, is notably smaller than the φ_{LMI} trend (Table S5). This implies that weak TCs contribute greatly to the poleward migration of WNP TCs, which is consistent with the finding of Zhan and Wang (2017). More importantly, the estimated φ_{DP} trends are statistically significant at the 95% confidence level during both RW and WS periods using various best track data sets. The time series of annual-mean φ_{DP} in the WNP shows a poleward migration trend before 1999; for example, the trend was 1.00° ± 0.85°/decade for the IBTrACS best track data (Figure 1a) during the RW period (Kosaka & Xie, 2013; Li et al., 2015; Meehl et al., 2014; Trenberth & Fasullo, 2014), when the observed SST in the tropical WNP increased by 0.19 ± 0.15 °C/decade^{-1} (see Figure S6). However, the poleward migration trend no longer existed and was even reversed after 1999 (Figure 1a); for example, the trend was −2.22° ± 1.19°/decade for the IBTrACS best track data during the recent WS period (Kosaka & Xie, 2013; Li et al., 2015; Meehl et al., 2014) as the SST in the tropical WNP remained almost unchanged (0.01 ± 0.11 °C/decade; see Figure S6). Therefore, the existing theory on the tropical expansion may explain the poleward shift of TCs over the WNP during the RW period due to similar trends of SST and φ_{DP}, but it does not provide an explanation for the equatorward migration of TCs over the WNP during the recent WS period due to large differences between SST and φ_{DP} trends. In addition, despite the controversy associated with the existence of the recent warming hiatus period (Karl et al., 2015), the observed SST indeed underwent a WS period at least in the tropical WNP.

3.2. Possible Mechanisms for the Meridional Shift of TCs Over the WNP

For a TC, its φ_{DP} depends on TC genesis location that gives the TC initial latitude (φ_G), on TC intensity evolution that directly affects TC destructive potential and thus φ_{DP} during its lifetime, and on TC track pattern that determines its path and thus φ_{DP} during its lifetime. Interdecadal variability of φ_G is found to be closely related to interdecadal fluctuation of φ_{LMI} (Song & Klotzbach, 2018) and thus is assumed to be correlated with that of φ_{DP}. Moreover, the potential intensity (PI) is a known major factor controlling TC intensity evolution (Emanuel, 1999), which describes the thermodynamically based maximum TC intensity that the environment will support and thus connects closely to TC genesis and intensification. Furthermore, the WNP TCs are usually steered by the large-scale environmental flow, especially the flow in the main TC activity region of (15–25°N, 120–140°E; Chan & Gray, 1982; Sun et al., 2015). Thereby, the changes of φ_G, PI, and the large-scale environmental flow are expected to contribute greatly to the change of φ_{DP} during the RW and WS periods.

The RW and the recent WS were characterized by different regional SST patterns (Kosaka & Xie, 2013), which are supposed to play important roles in determining both PI spatial distribution and the large-scale environmental flow in the main TC activity region (15–25°N, 120–140°E) and eventually φ_{DP} of the TCs over the WNP. For instance, the mean SST in the tropics after 1999 remained unchanged (Figure S6), while φ_{DP}

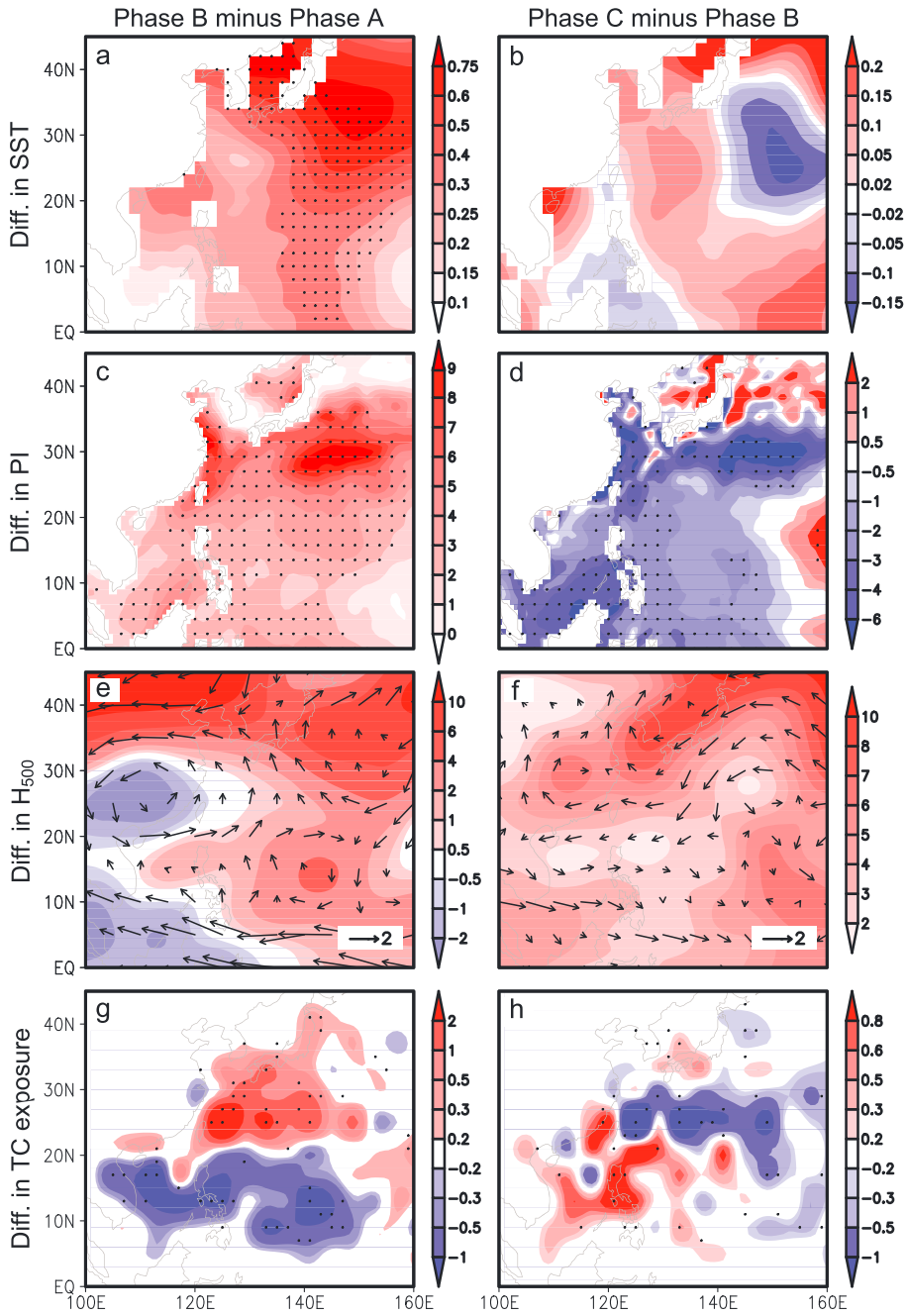

Figure 2. Differences in annual June–October mean SST, PI, large-scale circulation, and TC exposure among the three phases (Phases A, B, and C). (a, b) SST (°C). (c, d) PI (m/s). (e, f) The 500-hPa geopotential height (shading; m) and 850- to 300-hPa vertical-mean wind (vector; m/s^{-1}) and (g, h) TC exposure (number of days of exposure per year per 4° × 4°bin) based on the IBTrACS best track data set. Stippling in Figures 2a–2d (2g and 2h) denotes that the difference is significant at or above the 95% (90%) confidence level by the Student's *t* test. SST = sea surface temperature; PI = potential intensity; TC = tropical cyclone; IBtrACS = International Best Track Archive for Climate Stewardship.

decreased significantly (Figure 1), which implies that, rather than uniform SST change, it was the regional pattern of SST change that contributed greatly to the equatorward shift of the TCs over the WNP. However, little is known about the impact of regional patterns of RW and WS periods on TC migration. In the following sections, we focus on regional patterns in the RW and WS periods, including regional patterns of SST, PI, large-scale circulation, and TC exposure.

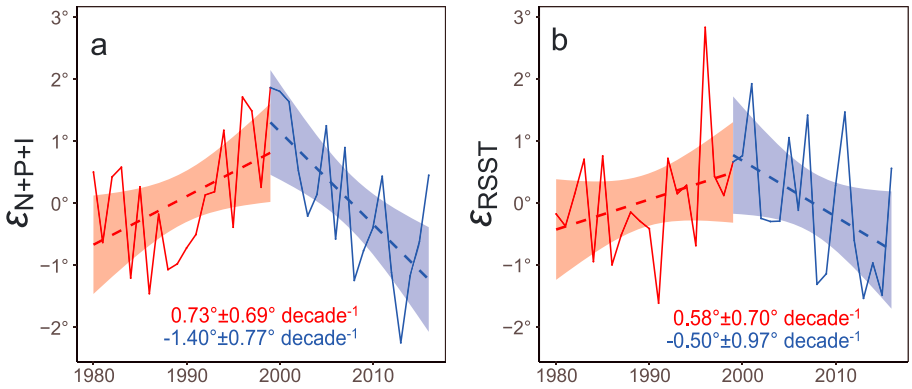

Figure 3. Contributions of the known dominant natural variability and relative SST variability to TC migration during the RW (red color) and WS (blue color) periods. Same as Figure 1a, except for the time series of φ_{DP} with ENSO, PDO, and IPO variability reduced (a) and of φ_{DP} with relative SST variability reduced (b). The values are calculated from the residuals of multivariate regression of φ_{DP} onto the June–October mean Niño-3.4, PDO, and tripole IPO indices and from the residuals of the single-variate regression of φ_{DP} onto the June–October mean relative SST variability. Linear trends (dashed lines) are shown with their 95% two-sided confidence intervals (shading), which are also quantitatively presented (annotated values). SST = sea surface temperature; TC = tropical cyclone; RW = rapid warming; WS = warming slowing-down; ENSO = El Niño–Southern Oscillation; PDO = Pacific Decadal Oscillation; IPO = Interdecadal Pacific Oscillation.

To investigate the causes for increasing (decreasing) trend of φ_{DP} during the period of 1980–1999 (of 1999–2016; Figure 1), we classify the phase of 1981–1990 as Phase A when φ_{DP} was at a relatively low level, the phase of 1994–2003 as Phase B when φ_{DP} reached its peak level, and the phase of 2006–2015 as Phase C when φ_{DP} fell back to a relatively low level. Comparison between φ_G and φ_{DP} indicates that despite their strong correlation (Table S6), φ_G is not the key factor contributing to the WNP TC migrations during the past decades, especially for the WS period, as nonsignificant differences in time-averaged φ_G cannot be used to effectively explain the significant differences in time-averaged φ_{DP} among the three phases (Phases A, B, and C; Figure S7) and φ_G also cannot be used to explain the recent reversal in the poleward shift of WNP TCs during the WS period (Table S7). To further investigate the linkage between global warming and WNP TC migration, we compare SST, PI, large-scale circulation, and TC exposure during the three phases (Figures 2 and S8). From Phase A to Phase B, the observed SST increased inhomogeneously over the WNP under global warming with a relatively warm SST pool to the southeast of Japan (Figure 2a). On the one hand, such a warm SST pool resulted in an increase of PI in the midlatitudes (about 20–40°N; Figure 2c), which contributed to the poleward migration of φ_{DP} through strong positive meridional (south-to-north) gradient of PI over the main TC activity region. Note that among the contributing factors (i.e., SST, outflow temperature, moisture, and the other factors) suggested by Emanuel (1999; see equation 1 in his paper), it is the SST increase that played a dominate role (86.2%) in determining the increase of PI from Phase A to Phase B (Table S8). On the other hand, under the hydrostatic constraint, such a pattern of SST change could induce relatively warm high-pressure anticyclone anomalies over the warm SST pool, which expanded to the western edge region of the western Pacific subtropical high and led to the westward expansion of the western Pacific subtropical high in the main TC activity region (Figure 2e). This led to remarkable southerly wind with the magnitude of about 0.5 m/s in the main TC activity region, which was favorable for the northward moving TCs over the WNP. As a result, under the joint contribution of increased PI in the midlatitudes and enhanced northward large-scale environmental flow, φ_{DP} moved poleward remarkably (Figure 2g). Moreover, consistent with the results of previous studies (Kossin et al., 2016, 2014; Wu & Wang, 2004), TC exposure increased significantly north of ~20°N but decreased distinctly in the south. The TC exposure increased in the regions of Taiwan, the Ryukyu Islands, Japan, and South Korea and decreased in the regions of Fujian province of China, Vietnam, and the Philippines (Figure 2g).

The situation became substantially different from Phase B to Phase C when the warming hiatus occurred. The SST changed to a nearly opposite pattern from Phase B to Phase C compared to that from Phase A to Phase B, with a spatial correlation coefficient of −0.91 (Figures 2a and 2b). On the one hand, the relatively cold SST pool, together with relatively warm outflow temperature at 200 hPa (Figure S9b), contributed to the

Table 1
Linear Trends of Annual-Mean φ_{DP} and Their Regression Residuals During RW and WS Periods

Index	RW period (1980–1999)	WS period (1999–2016)	Whole period (1980–2016)
φ_{DP}	1.00 ± 0.85	−1.81 ± 1.16	0.16 ± 0.40
$\varepsilon_{Niño\text{-}3.4}$	0.98 ± 0.76	−1.37 ± 0.81	0.18 ± 0.35
R^2, p value	0.16, 0.085	0.47, 0.002	0.24, 0.002
ε_{PDO}	0.79 ± 0.70	−1.41 ± 1.10	−0.04 ± 0.35
R^2, p value	0.34, 0.007	0.21, 0.055	0.25, 0.002
ε_{IPO}	0.84 ± 0.72	−1.39 ± 0.79	−0.04 ± 0.33
R^2, p value	0.27, 0.017	0.48, 0.001	0.34, <0.001
ε_{N+P+I}	0.73 ± 0.69	−1.40 ± 0.77	−0.07 ± 0.32
R^2, p value	0.37, 0.055	0.49, 0.022	0.35, 0.002
ε_{RSST}	0.58 ± 0.70	−0.50 ± 0.97	−0.04 ± 0.31
R^2, p value	0.41, 0.003	0.55, <0.001	0.40, <0.001

Note. Listed are WNP TC migration rate and 95% confidence interval (°/decade) of annual-mean φ_{LMI} and the residuals of the regression of φ_{DP} onto the annual June–October mean Niño-3.4, PDO, IPO, and relative SST indices (i.e., $\varepsilon_{Niño\text{-}3.4}$, ε_{PDO}, ε_{IPO}, and ε_{RSST}), along with the residuals of the trivariate regression of φ_{DP} onto the Niño-3.4, PDO, and tripole IPO indices (i.e., ε_{N+P+I}) using the IBTrACS best track data. For the single-variate and trivariate regressions, the variance explained R^2 and p value are also given. RW = rapid warming; WS = warming slowing-down; WNP = western North Pacific; TC = tropical cyclone; PDO = Pacific Decadal Oscillation; IPO = Interdecadal Pacific Oscillation; SST = sea surface temperature; IBtrACS = International Best Track Archive for Climate Stewardship.

decrease of PI in the midlatitudes over the main TC activity region, which contributed to the equatorward migration of φ_{DP} through strong negative meridional (south-to-north) gradient of PI over the main TC activity region (Figure 2d). Moreover, it was the SST that contributed mainly (69.3%) to the change of PI among the contributing factors (Table S8). On the other hand, due to the relatively cold SST pool to the southeast of Japan and its extension, a relatively low pressure surrounding a cyclonic circulation occurred over the cold pool and expanded to the main TC activity region. This led to remarkable northerly wind with a magnitude of about 0.7 m/s in the main TC activity region, which was favorable for the southward moving of the TCs over the WNP (Figure 2f). Thereby, it is the decreased PI in the midlatitudes and the enhanced southward large-scale environmental flow that accounted for not only the equatorward shift of φ_{DP} but also the reversed pattern of changes in TC exposure, for example, the TC exposure increased in Fujian of China, Taiwan, and the Philippines and decreased around the Ryukyu Islands and South Korea (Figure 2h).

4. Discussion

The most distinctive feature of the aforementioned SST change pattern is the increase (decrease) of the SST and thus relatively warm (cold) SST pool over the key region of (20–40°N, 140–160°E) during the RW period (the WS period). Our results show that φ_{DP} was also closely related to the SST over the key region, which exhibited a high correlation with the trend of φ_{DP} during all three periods (i.e., the RW period, the WS period, and the whole period of 1980–2016; Figure S10). Moreover, as mentioned above, rather than the SST itself, it is the SST gradient and thus relative SST (defined below) that contributed to the changes of PI and large-scale environmental flow, which eventually led to TC migration trend. Thereby, to further investigate the relationship between SST change and TC migration trend, we introduce the concept of relative SST, which is defined as the difference between the SST averaged over the key region (20–40°N, 140–160°E) and the SST averaged over the tropics and subtropics (40°S to 40°N) globally (Figure S11).

To test the importance of relative SST for φ_{DP}, we compare the contributions of relative SST and the three known dominant modes of variability (i.e., ENSO, PDO, and IPO) to φ_{DP} by regressing the time series of φ_{DP} onto these indices (Figure 3 and Table 1). Relative SST explains remarkably large percentage of the variability of the annual-mean φ_{DP} time series, more than the combination of ENSO, PDO, and IPO during the RW and WS periods, respectively. More importantly, the residual of the trivariate regression of ENSO, PDO, and IPO maintains a significant poleward (equatorward) migration trend of 0.73° ± 0.69° (−1.40° ± 0.77°)/decade, while the residual of the single-variate regression of relative SST shows a smaller and insignificant poleward (equatorward) migration trend of 0.58° ± 0.70° (−0.50° ± 0.97°)/decade (Figure 3 and Table 1). Therefore, compared with the theory based on the anthropogenic forcing and the known dominant modes of variability (Kossin et al., 2016, 2014; Murakami et al., 2012; Wu et al., 2014), the mechanism associated with the regional pattern of SST change characterized by a relatively warm or cold SST pool is a more convincing explanation for the migration trend of the TCs over the WNP since 1980, especially for the recent WS period. This implies but does not necessary mean that the anthropogenic factors did not contribute significantly to the WNP TC migration trend as expected, since it is difficult to distinguish the contributions of relative SST variability and anthropogenic forcing based on the short time series. In addition, according to the wavelet analysis of relative SST (Figure S12), the change of relative SST was probably due to natural internal variability with a long period (40–60 years) rather than to the IPO or global warming, which is being investigated currently.

Acknowledgments
Data supporting Figures and are available as supporting information Data Sets S1 and S2. The authors thank two anonymous reviewers for their constructive comments that helped improve the manuscript. This work is sponsored by the National Key Research Project (2017YFA0603802 and 2015CB453200), the National Natural Science Foundation of China (grants 41630423, 41875069, 41605072, 41430426, and 41675077), National Science Foundation (AGS 16-43297), NOAA (grant NA18OAR4310298), the Priority Academic Program Development of Jiangsu Higher Education Institutions (PAPD), and the Natural Science Foundation of Jiangsu Province (grant BK20160768). We thank James P. Kossin and Suzana J. Camargo for their valuable suggestions.

References

Allen, R. J., Sherwood, S. C., Norris, J. R., & Zender, C. S. (2012). Recent Northern Hemisphere tropical expansion primarily driven by black carbon and tropospheric ozone. *Nature*, *485*(7398), 350–354. https://doi.org/10.1038/nature11097

Cardona, O. D., van Aalst, M. K., Birkmann, J., Fordham, M., McGregor, G., Perez, R., et al. (2012). Determinants of risk: Exposure and vulnerability. In C. B. Field, et al. (Eds.), *Managing the risks of extreme events and disasters to advance climate change adaptation* (pp. 65–108). Cambridge, UK and New York: Cambridge University Press.

Chan, J. C. L., & Gray, W. M. (1982). Tropical cyclone movement and surrounding flow relationships. *Monthly Weather Review*, *110*(10), 1354–1374. https://doi.org/10.1175/1520-0493(1982)110<1354:TCMASF>2.0.CO;2

Chan, J. C. L., & Shi, J. (1996). Long-term trends and interannual variability in tropical cyclone activity over the western North Pacific. *Geophysical Research Letters*, *23*(20), 2765–2767. https://doi.org/10.1029/96GL02637

Dee, D. P., Uppala, S. M., Simmons, A. J., Berrisford, P., Poli, P., Kobayashi, S., et al. (2011). The ERA-Interim reanalysis: Configuration and performance of the data assimilation system. *Quarterly Journal of the Royal Meteorological Society*, *137*(656), 553–597. https://doi.org/10.1002/qj.828

Emanuel, K. A. (1999). Thermodynamic control of hurricane intensity. *Nature*, *401*(6754), 665–669. https://doi.org/10.1038/44326

Emanuel, K. A. (2005). Increasing destructiveness of tropical cyclones over the past 30 years. *Nature*, *436*(7051), 686–688. https://doi.org/10.1038/nature03906

Fyfe, J. C., Gillett, N. P., & Zwiers, F. W. (2013). Overestimated global warming over the past 20 years. *Nature Climate Change*, *3*(9), 767–769. https://doi.org/10.1038/nclimate1972

Henley, B. J., Gergis, J., Karoly, D. J., Power, S., Kennedy, J., & Folland, C. K. (2015). A tripole index for the Interdecadal Pacific Oscillation. *Climate Dynamics*, *45*(11-12), 3077–3090. https://doi.org/10.1007/s00382-015-2525-1

Kalnay, E., Kanamitsu, M., Kistler, R., Collins, W., Deaven, D., Gandin, L., et al. (1996). The NCEP/NCAR 40-year reanalysis project. *Bulletin of the American Meteorological Society*, *77*(3), 437–471. https://doi.org/10.1175/1520-0477(1996)077<0437:TNYRP>2.0.CO;2

Karl, T. R., Arguez, A., Huang, B., Lawrimore, J. H., McMahon, J. R., Menne, M. J., et al. (2015). Possible artifacts of data biases in the recent global surface warming hiatus. *Science*, *348*(6242), 1469–1472. https://doi.org/10.1126/science.aaa5632

Kim, J.-H., Brown, S. J., & McDonald, R. E. (2011). Future changes in tropical cyclone genesis in fully dynamic ocean- and mixed layer ocean-coupled climate models: A low-resolution model study. *Climate Dynamics*, *37*(3-4), 737–758. https://doi.org/10.1007/s00382-010-0855-6

Knapp, K. P., Kruk, M. C., Levinson, D. H., Diamond, H. J., & Neumann, C. J. (2010). The international best track archive for climate stewardship (IBTrACS): Unifying tropical cyclone data. *Bulletin of the American Meteorological Society*, *91*(3), 363–376. https://doi.org/10.1175/2009BAMS2755.1

Knapp, K. R., & Kruk, M. C. (2010). Quantifying interagency differences in tropical cyclone best track wind speed estimates. *Monthly Weather Review*, *138*(4), 1459–1473. https://doi.org/10.1175/2009MWR3123.1

Knutson, T. R., McBride, J. L., Chan, J., Emanuel, K., Holland, G., Landsea, C., et al. (2010). Tropical cyclones and climate change. *Nature Geoscience*, *3*(3), 157–163. https://doi.org/10.1038/ngeo779

Kosaka, Y., & Xie, S.-P. (2013). Recent global-warming hiatus tied to equatorial Pacific surface cooling. *Nature*, *501*(7467), 403–407. https://doi.org/10.1038/nature12534

Kossin, J. P., Emanuel, K. A., & Camargo, S. J. (2016). Past and projected changes in western North Pacific tropical cyclone exposure. *Journal of Climate*, *29*(16), 5725–5739. https://doi.org/10.1175/JCLI-D-16-0076.1

Kossin, J. P., Emanuel, K. A., & Vecchi, G. A. (2014). The poleward migration of the location of tropical cyclone maximum intensity. *Nature*, *509*(7500), 349–352. https://doi.org/10.1038/nature13278

Kruk, M. C., Knapp, K. R., & Levinson, D. H. (2010). A technique for combining global tropical cyclone best track data. *Journal of Atmospheric and Oceanic Technology*, *27*(4), 680–692. https://doi.org/10.1175/2009JTECHA1267.1

Lee, T.-C., Knutson, T. R., Kamahori, H., & Ying, M. (2012). Impact of climate change on tropical cyclones in the western North Pacific Basin. Part I: Past observations. *Tropical Cyclone Research and Review*, *1*, 213–230.

Li, Q., Yang, S., Xu, W., Wang, X. L., Jones, P., Parker, D., et al. (2015). China experiencing the recent warming hiatus. *Geophysical Research Letters*, *42*, 889–898. https://doi.org/10.1002/2014GL062773

Liu, K. S., & Chan, J. C. L. (2008). Interdecadal variability of western North Pacific tropical cyclone tracks. *Journal of Climate*, *21*(17), 4464–4476. https://doi.org/10.1175/2008JCLI2207.1

Mantua, N. J., Hare, S. R., Zhang, Y., Wallace, J. M., & Francis, R. C. (1997). A Pacific interdecadal climate oscillation with impacts on salmon production. *Bulletin of the American Meteorological Society*, *78*(6), 1069–1079. https://doi.org/10.1175/1520-0477(1997)078<1069:APICOW>2.0.CO;2

Meehl, G. A., Teng, H., & Arblaster, J. M. (2014). Climate model simulations of the observed early-2000s hiatus of global warming. *Nature Climate Change*, *4*(10), 898–902. https://doi.org/10.1038/nclimate2357

Murakami, H., Wang, Y., Yoshimura, H., Mizuta, R., Sugi, M., Shindo, E., et al. (2012). Future changes in tropical cyclone activity projected by the new high-resolution MRI-AGCM. *Journal of Climate*, *25*(9), 3237–3260. https://doi.org/10.1175/JCLI-D-11-00415.1

Peduzzi, P., Chatenoux, B., Dao, H., De Bono, A., Herold, C., Kossin, J., et al. (2012). Tropical cyclones: Global trends in human exposure, vulnerability and risk. *Nature Climate Change*, *2*(4), 289–294. https://doi.org/10.1038/nclimate1410

Rayner, N. A., Parker, D. E., Horton, E. B., Folland, C. K., Alexander, L. V., Rowell, D. P., et al. (2003). Global analyses of sea surface temperature, sea ice, and night marine air temperature since the late nineteenth century. *Journal of Geophysical Research*, *108*(D14), 4407. https://doi.org/10.1029/2002JD002670

Smith, T. M., & Reynolds, R. W. (2003). Extended reconstruction of global sea surface temperatures based on COADS data (1854–1997). *Journal of Climate*, *16*(10), 1495–1510. https://doi.org/10.1175/1520-0442-16.10.1495

Song, J., & Klotzbach, P. J. (2018). What has controlled the poleward migration of annual averaged location of tropical cyclone lifetime maximum intensity over the western North Pacific since 1961? *Geophysical Research Letters*, *45*, 1148–1156. https://doi.org/10.1002/2017GL076883

Sun, Y., Zhong, Z., Yi, L., Li, T., Chen, M., Wan, H., et al. (2015). Dependence of the relationship between the tropical cyclone track and western Pacific subtropical high intensity on initial storm size: A numerical investigation. *Journal of Geophysical Research: Atmospheres*, *120*, 11,451–11,467. https://doi.org/10.1002/2015JD023716

Trenberth, K. E., & Fasullo, J. T. (2014). An apparent hiatus in global warming. *Earth's Future*, *1*, 19–32.

Wang, R., Wu, L., & Wang, C. (2011). Typhoon track changes associated with global warming. *Journal of Climate*, *24*(14), 3748–3752. https://doi.org/10.1175/JCLI-D-11-00074.1

Wu, L., Chou, C., Chen, C. T., Huang, R., Knutson, T. R., Sirutis, J. J., et al. (2014). Simulations of the present and late-twenty-first-century western North Pacific tropical cyclone activity using a regional model. *Journal of Climate*, *27*(9), 3405–3424. https://doi.org/10.1175/JCLI-D-12-00830.1

Wu, L., & Wang, B. (2004). Assessing impacts of global warming on tropical cyclone tracks. *Journal of Climate*, *17*(8), 1686–1698. https://doi.org/10.1175/1520-0442(2004)017<1686:AIOGWO>2.0.CO;2

Yang, L., Du, Y., Wang, D., Wang, C., & Wang, X. (2015). Impact of intraseasonal oscillation on the tropical cyclone track in the South China Sea. *Climate Dynamics*, *44*(5-6), 1505–1519. https://doi.org/10.1007/s00382-014-2180-y

Ying, M., Knuston, T. R., Kamahori, H., & Lee, T.-C. (2012). Impacts of climate change on tropical cyclones in the western North Pacific basin. Part II: Late twenty-first century projections. *Tropical Cyclone Research and Review*, *1*, 231–241.

Yokoi, S., & Takayabu, Y. N. (2009). Multi-model projection of global warming impact on tropical cyclone genesis frequency over the western North Pacific. *Journal of the Meteorological Society of Japan*, *87*(3), 525–538. https://doi.org/10.2151/jmsj.87.525

Zhan, R., & Wang, Y. (2017). Weak tropical cyclones dominate the poleward migration of the annual mean location of lifetime maximum intensity of northwest Pacific tropical cyclones since 1980. *Journal of Climate*, *30*(17), 6873–6882. https://doi.org/10.1175/JCLI-D-17-0019.1